POLITECNICO DI TORINO
Repository ISTITUZIONALE

A Finite Element approach for the prediction of the mechanical behaviour of layered composites produced by Continuous Filament Fabrication ({CFF})

(Article begins on next page)

24 April 2024

A finite element approach for the prediction of the mechanical behaviour of layered composites produced by Continuous Filament Fabrication (CFF)

Manuela Galati , Marco Viccica [*], Paolo Minetola

Integrated Additive Manufacturing Center (IAM) Politecnico di Torino, Department of Management and Production Engineering (DIGEP), Torino, Italy

ARTICLE INFO

ABSTRACT

Continuous Filament Fabrication (CFF) is the additive manufacturing process for producing material reinforced with long fibres. Differently from other processes, CFF allows producing components in composite materials without using tools, moulds or post-processing operations and with a strengthened area only where it is strictly required. This innovative way of producing composites makes a new design approach necessary for better exploitation of the material. This work presents a preliminary study based on 3D Finite Element (FE) method to predict the mechanical behaviour of composite materials fabricated by CFF. With this aim, a FE model is developed to determine the actual material properties in terms of longitudinal, transverse and shear modulus. Comparisons between experimental and numerical tensile results at different fibre orientations validate the model. The robustness of the proposed approach is confirmed by the comparison with the experimental characterisation of composites produced with two different fibre reinforcements, Carbon and Kevlar®.

1. Introduction

Composites consist of two or more materials combined in a new one with improved properties [1]. In engineering, polymer-based composite materials, also called fibre reinforced polymers (FRPs) are considered one of the best composite solutions because of their relatively high strength and low weight [2]. Nowadays the use of FRPs is consolidated in several fields such as military and civil aircraft construction (e.g. wings, fuselages and other secondary internal parts) [3], automotive industry (e.g. roof and body panels, hidden structural parts) [4], naval ships and submarines (e.g. decks, bulkheads, propellers, machinery, and other equipment) [5] and civil industry (e.g. structural shapes, bridge decks, building structures) [6,7].

FRPs consist of a polymer matrix which embeds the fibres as the reinforcing phase. The arrangement and the orientation of the fibres, their concentration and distribution have a strong influence on the final properties of the composite. Most of the conventional processes for composite components require the use of prepregs, that is sheets of woven fabric or unidirectional fibres. In prepregs, the fibres are pre-impregnated in a resin matrix, that is usually epoxy [8]. The components are then shaped using specific tools and moulds. Other conventional industrial manufacturing processes for FRP components are Automatic tape layers/laying (ATLs) [3], vacuum moulding (VM) [9],

resin transfer moulding (RTM) [10], vacuum-assisted RTM (VARTM) [11], resin film infusion (RFI) [12] and low-temperature moulding (LTM) [13]. During the last decades, additive manufacturing (AM) approach has also been adopted to produce component made by composite materials [14]. The most common techniques are stereolithography (SLA), laminated object manufacturing (LOM), selective laser sintering (SLS) and fused deposition modelling (FDM). SLA is based on the polymerisation of a photosensitive resin. The reaction is activated by an ultraviolet laser which selectively cures the resin stocked in a vat [15]. Adding fibres in the resin showed an increase in the mechanical properties of components. However, manufacturing issues, such as the weak interface adhesion between the reinforcement and the resin [16] and carbon fibre opaqueness to the UV light [17], limit the production of functional components. The LOM process is similar to the conventional processes because it uses sheets of an epoxy matrix reinforced with unidirectional and continuous glass fibres. A 3D part is sequentially obtained laying and laminating adhesive-coated sheets which are cut by a laser beam [18]. Researchers from Kansas State University developed a novel variant of LOM which uses pre-preg tape and a CO_2 laser beam [19]. When compared to traditional LOM, that method presented waste reduction, good interfacial bonding and increased mechanical properties. In the SLS process, the thermal energy of a laser beam selectively sinters, i.e. melts, polymer powders [20]. To produce a composite by

---

SLS, Zhu et al. [21] developed a three-dimensional co-continuous carbon fibres/PA12/epoxy resin (CF/PA12/EP) ternary structure. After the SLS process, the CF/PA12 material is porous and needs to be infiltrated with the thermosetting EP under a high temperature and a negative pressure; finally, the part is cured. Composite materials made by SLS can be also obtained mixing a reinforced material in short form directly in the polymeric powder. FDM is an extrusion process by which a polymeric filament is melted and deposited on the previous layer through a heated nozzle [15]. Zhong et al. [22] printed an ABS filament reinforced with short glass fibres which showed a significantly enhanced strength. Spoerk et al. [23] demonstrated that the FDM process can be an easy route to fabricate aligned short carbon fibre-filled polypropylene composites with anisotropic mechanical properties and thermal conductivity. All these AM techniques allow reinforcing the polymeric matrix with short fibres only. Recently, Markforged Inc. [24] has patented a new FDM process, named Continuous Filament Fabrication (CFF) process, that allows laying continuous-fibre reinforcements coated and embedded in a thermoplastic matrix. Therefore, CFF is the only AM process for producing components reinforced by long fibres.

1.1. Continuous Filament Fabrication (CFF) process

The CFF system has a print head that is composed of two nozzles for extruding the PA matrix and the reinforcement fibre, respectively.

The height of the printed layer is defined by the motion of the print bed in the Z-direction. The print head deposits the materials by moving across the XY plane. The print head is equipped with two nozzles that extrude the matrix and the fibre reinforcement respectively. The matrix materials are Nylon (PA12) or Onyx which is a nylon filament pre-reinforced with short fibres of carbon. There are four types of reinforcements which are Carbon Fibre (CF), Fiberglass (FG), Kevlar® (KV) and high-strength high-temperature (HSHT) fiberglass. The reinforcement fibre is encapsulated in a polymeric matrix. Both nozzles are heated up to the softening temperature of the nylon for easy deposition of the materials after extrusion. Within the single layer, the reinforcement filament is deposited continuously according to a predefined path that depends on the deposition strategy. The fibre covers the entire area to be reinforced without interruption and, in the end, a cutter positioned just above the deposition nozzle cuts the filament. The adhesion between the reinforcement filament and previous layer or the surrounding material is guaranteed by the polymeric matrix that encapsulates the

continuous fibre. The build job must be prepared in the proprietary Eiger software by Markforged, that is available in the cloud. The main settings of Eiger concern the material, the reinforcement, the layer height, the infill and the contour paths, i.e. walls. The matrix filament is laid with an angle of $\pm 45°$ with respect to the XY reference system on the build plate. For every reinforced layer, the user can choose the deposition strategy of the fibre. The reinforcement filament is laid either in a concentric infill path or in an isotropic one (Fig. 1). The isotropic infill path allows the user to define the angle of fibre deposition. Therefore, it is possible to produce layered parts with locally different mechanical properties.

Unlike traditional production methods for laminated fibre reinforced plastic (FRP), the innovation of the additive CFF process empowers engineers with much greater design freedom in tailoring the reinforcement to meet the desired part strength and performance. Economic and material savings for sustainability derive by the possibility to define in advance the number of reinforced layer and the fibre deposition strategy for CFF parts, which have a thermoplastic matrix.

However, at the moment, FE tools for the design of composite parts have been developed for pre-pegs and traditional lamination only. The absence of a specific FE tool for CFF parts is detrimental for the advantages of this additive technique. Without the possibility to predict the resulting mechanical performance of the part depending on the reinforcement strategy, a time-consuming and expensive trial and error approach should be adopted to produce a CFF part that meets design requirements and strength. Under-reinforcement generates material waste because the part cannot be used, whereas over-reinforcement implies excessive use of material and higher costs. Currently a spool of 900 cc of Nylon filament is sold at 170 €, while a spool of 150 cm³ of Carbon or Kevlar fibre costs 450 € and 300 € respectively.

2. State of the art of CFF modelling

Since CFF technology is rather new, research on the characterisation of long-fibre composites made by CFF is at an early stage. Preliminary studies highlighted that CFF composites might show a low interlaminar shear performance and a weak bond between the matrix and the reinforcement [25] which cause layer delamination [25] or the presence of voids [26]. Therefore, the obtained composite material may have weak mechanical proprieties. Additionally, the inclusion of air that may occur during the process [27] and moisture absorption by the PA (Nylon) matrix [28] can also decrease the tensile properties of the material. Van
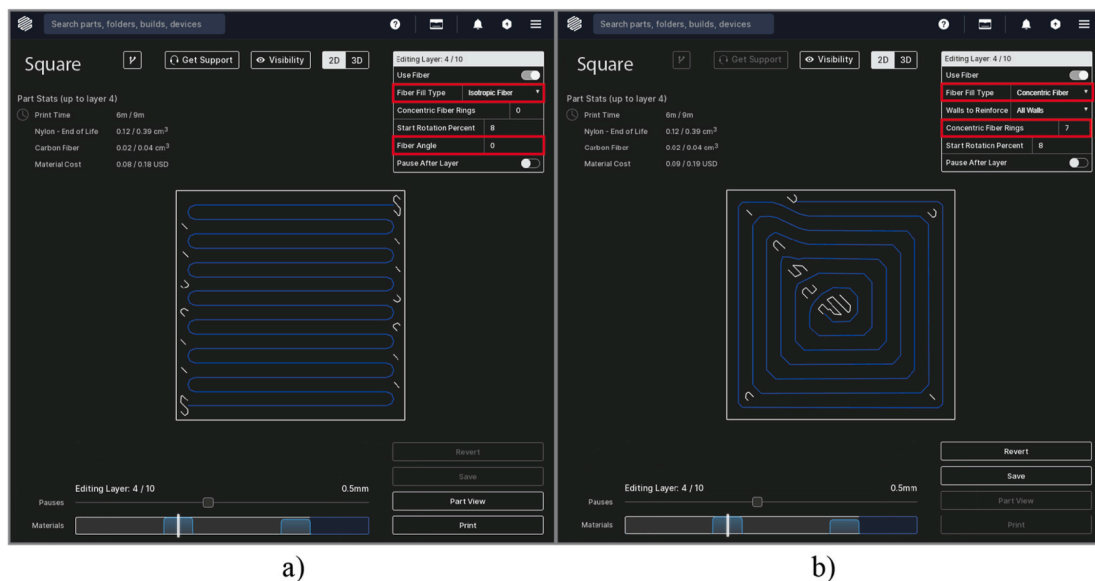

Fig. 1. Example of reinforcement strategy in Eiger software with isotropic infill path (a) and concentric infill path (b). The blue line indicates the path for the fibre filament. The white line shows the path of the matrix.

der Klift [26] evaluated the tensile properties of Carbon fibre reinforced thermoplastic (CFRTP) composites. The elastic modulus E_{cfr-L} of the layer reinforced with Carbon fibre (CF) was calculated using the rule of mixture of composites [29] considering the elastic modulus E_t of the composite and the one E_n of Nylon obtained by experimental tensile tests. The results showed that for a fewer number of CFRTP layers, E_{cfr-L} was equal to 231.4 GPa which is close to the value (230 GPa) of the TORAYCA® T300 tow made by TORAY® [30]. The same method was applied [27] to predict the layer tensile modulus E_{kfr-L} of Kevlar fibre-reinforced thermoplastic (KFRTP). Dickson obtained a value of about 83.7 GPa, which is comparable to the one (70.3 GPa) of Kevlar 29 yarns produced by DuPont [31]. Melenka et al. [32] evaluated the mechanical performance of KFRTP standard specimens [33] which were printed with 2, 4 or 5 reinforced concentric fibres rings (2R, 4R or 5R). The elastic modulus $E_{kfrtp-p}$ of a KFRTP was estimated using the volume average stiffness (VAS) method. The calculated values ($E_{kfrtp-p-2R} = 4.2$ GPa, $E_{kfrtp-p-4R} = 7.4$ GPa, $E_{kfrtp-p-5R} = 8.9$ GPa) showed a low deviation from the experimental ones ($E_{kfrtp-exp-2R} = 1.8$ GPa, $E_{kfrtp-exp-4R} = 6.9$ GPa, $E_{kfrtp-exp-5R} = 9$ GPa) only for the specimens with the highest fibres content. Abadi et al. [34] obtained similar results on samples printed according to ASTM D3039 [35] with different orientations of the fibre filament. The tested samples included both CF and Kevlar. The deposition strategy considered concentric and isotropic infill. The predicted values by VAS method ($E_{cfrtp-p} = 34.2$ GPa, $E_{kfrtp-p} = 8.4$ GPa) and the experimental ones ($E_{cfrtp-exp} = 37$ GPa, $E_{kfrtp-exp} = 8.7$ GPa) were comparable to the ones reported by Melenka [32]. Both methods [32,34] forecasted the longitudinal tensile properties only while in the literature the only study about an analytical prediction of the longitudinal modulus E_1, transverse modulus E_2 and the in-plane G_{12} shear modulus of the reinforced layer was conducted by Dutra [36]. In that research, each specimen consisted of two nylon layers on the top and of six CFRTP layers on the bottom. The fibre filament was deposited at 0°, 90°, ±45° for the longitudinal, transverse and in-plane shear specimens, respectively. The comparison between the estimated values by the applied mathematical method, namely asymptotic homogenisation, and the experimental ones showed a large deviation, especially for the transverse and in-plane shear modulus. Dutra attributed the resulting deviation to the differences in mechanical properties between the thermoplastic matrix embedding the fibre filament and the pure nylon filament. Todoroki et al. in Ref. [37] investigated the effect of the folded fibre filament generated by the path inversion during deposition. The experimental campaign included samples printed with the CF at 0°, 90°, and ±45°. The geometry was extracted from Ref. [26] and scaled up and the side edges were cut to remove the folded fibre filament. Tensile tests showed lower stiffness than the specimens produced with the folded fibre filament included in the analysis. However, real parts printed by the CFF process will not exhibit such an extreme behaviour because the removal of the folded fibre filament is not a common practice that Markforged suggests. Moreover, the CFF process requires that the fibres are embedded in the polymeric matrix not to cause hazards to human health in the case of damage with direct exposition of the fibres. Heavy damage of the fibres also jeopardize the part strength, while a defect in the polymer layers are less severe. Other approaches to evaluate the mechanical properties of composite specimens are based on the use of finite element (FE) models which can simulate and predict the real component behaviour. For composite made of forming plies by traditional manufacturing processes, 2D FE models are used. For composite produced by CFF process, Abadi [34] developed a 2D FE analysis by modelling each layer with quadrilateral shell elements. That FE model can reasonably estimate the specimen failure modes and the criteria of their damage initiation. Nevertheless, the approach can work well when the simulated components correspond to the shell definition for which planar dimensions are more relevant than the thickness. CFF manufactured part are instead 3D components and therefore 3D models are required to well simulate the real behaviour of components which do not comply with the shell definition. In this sense,

Van Der Klift [38] developed a 3D-FE model to simulate the behaviour of tensile specimens printed on a MarkTwo printer. Van Der Klift modelled the nylon as a homogenous isotropic solid material while an orthotropic solid model was used for the CF reinforcement embedded in the matrix. The input material properties were set according to his previous work [26]. The numerical results of the tensile test simulation over-estimated the numerical results of about 53%.

When compared to the existing literature, an innovative 3D numerical model for the CFF process is implemented in this work with the aim of determining the equivalent mechanical properties with higher accuracy of layered CFF composites with reinforcement fibres deposited in any direction.

The proposed approach is based on the tensile test results of specimens reinforced with three different orientations of the fibres. These experimental results represent the key to calibrate the model. The novel model is tested on both Carbon and Kevlar reinforcements with a nylon matrix. Once the model is calibrated, its prediction capability and accuracy are evaluated for different fibre orientation in the tensile specimen by comparison with the experimental results.

3. Methodology

The development of a FE model, which can emulate the mechanical behaviour of a composite material reinforced with fibre deposited in any direction, requires the evaluation of the longitudinal elastic modulus E_1, the transverse elastic modulus E_2, and the in-plane shear modulus G_{12} to be assigned to the reinforced layer. To this aim, a specific fibre deposition is exploited in the fabrication of the tensile specimen to get a mechanical behaviour that is primarily dominated by a unique material property and a single modulus. For instance, if the fibre is deposited along the tensile load direction, the longitudinal elastic modulus E_1 contributes the most to the mechanical behaviour of the specimen. Similarly, the mechanical behaviour of the specimens reinforced with the fibre deposited at 90° and 45° with respect to the tensile load direction are more influenced by the transversal modulus E_2 and the in-plane shear modulus G_{12} respectively.

Therefore, the application of the proposed FE methodology requires the production of four types of specimens. A specimen of pure nylon is produced with the standard deposition strategy to calibrate the properties of the thermoplastic matrix. The other three types of tensile samples are manufactured with only one central layer reinforced with the fibre deposited at 0, 45 and 90° respectively. The direction of the tensile load is assumed as the reference one, thus the specimen with the reinforcement oriented at zero degrees is expected to exhibit the highest strength. After the production of the specimen, the tensile test is carried out and the load-displacement curve is recorded. The experimental results are used to calibrate the 3D FE model of the composite specimens according to the workflow in Fig. 2. The developed model consists of a set of layers bonded to each other to mimic the experimental condition on the real tensile specimen. The number of layers and the layer thickness in the FE model are the same of the 3D printed specimen. The polymer matrix is simulated as an isotropic and homogenous material, while the continuous fibre filament is simulated as a homogenous and orthotropic material. Initially, the material properties in the model of the pure-nylon specimen are set following the material datasheet by Markforged [39]. The FE analysis allows estimating the maximum longitudinal displacement ($u_{max,num}$) under a predefined load. At this point, the tensile properties of the matrix material are modified iteratively up to the convergence between the numerical ($u_{max,num}$) and the experimental ($u_{max,exp}$) results. The convergence is considered valid for a maximum deviation of 10% between $u_{max,num}$ and $u_{max,exp}$.

Once the matrix proprieties are defined, the 3D FE is modified to emulate the mechanical behaviour of the fibre deposited at 0° for calibrating the value of the longitudinal modulus E_1 of the reinforcement fibre. To this the possibility to define a local material reference (LMR) system for the elements of the FE model is exploited. This LMR system
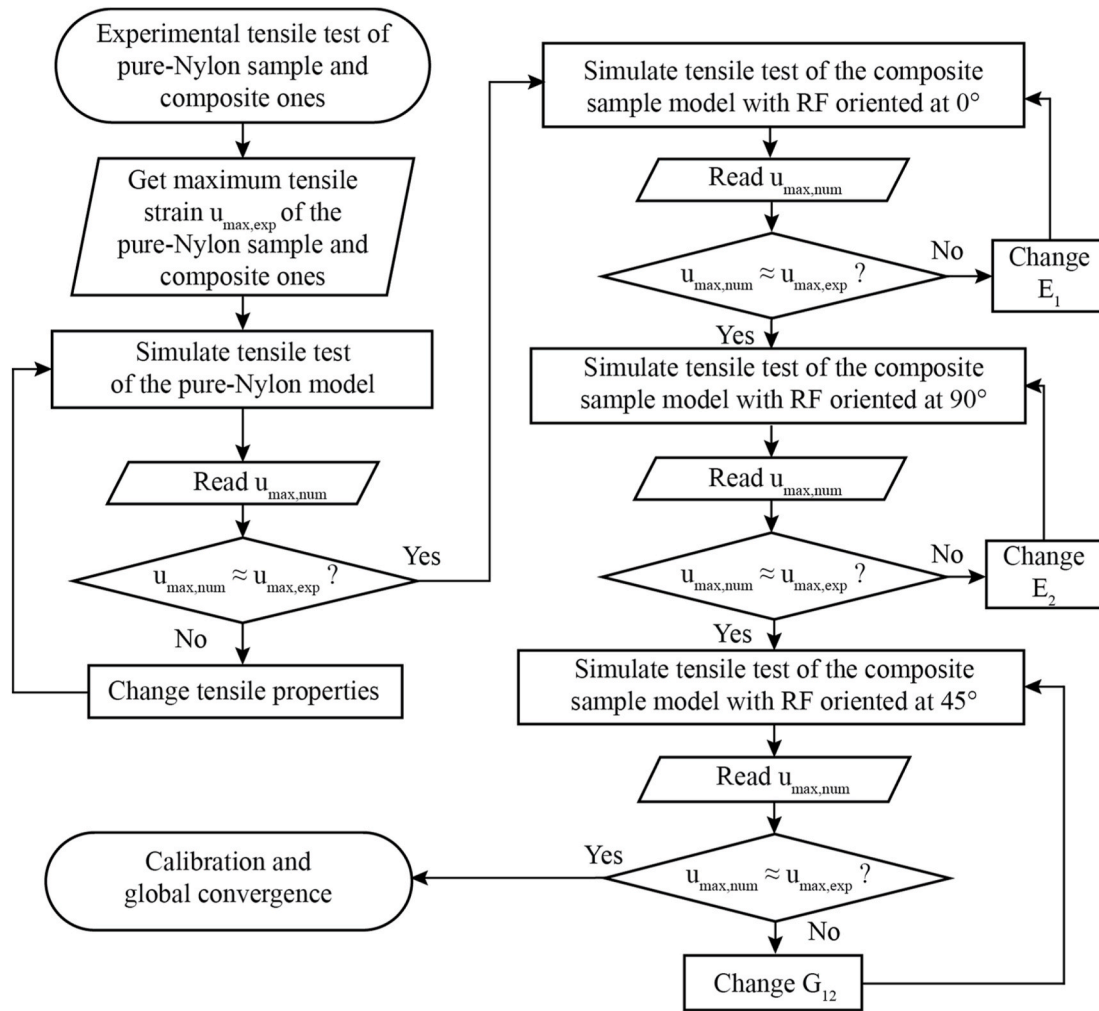
Fig. 2. Methodology workflow.

allows modelling the macroscopic behaviour of the specimen as the fibre orientation changes. The first axis of the LMR system is oriented along the deposition direction in the reinforcement layer, the second axis is perpendicular to the deposition direction within the layer, and the third axis is perpendicular to the deposition plane. As in the calibration of the matrix properties, at each iteration, only the value of the longitudinal modulus E_1 is iteratively changed until the simulated maximum displacement $u_{max,num}$ under a specific load is approximately equal to the experimental maximum displacement $u_{max,exp}$ of the corresponding real specimen with fibre oriented at zero degrees. The specimen produced with the fibre orientated at 90° is then used to calibrate the value of the transversal modulus E_2. For this purpose, the predetermined E_1 value is set and the 3D FE model is modified to simulate the corresponding fibre orientation. Then the value of the transversal modulus E_2 is iteratively changed until convergence between the numerical results and the experimental one. The same procedure is repeated for the specimen with the fibre oriented at 45° to calibrate the value of the in-plane shear modulus G_{12} with predetermined values of E_1 and E_2. Finally, a global numerical convergence is forced and the predetermined values of E_1 and E_2 are slightly modified to increase the matching between the experimental results and numerical ones for improved accuracy of the FE model.

4. Materials and equipment

For this study, the geometry of the tensile specimen (Fig. 3) is designed according to the Type II of the ASTM D638 guideline [33]. The standard dimensions of the specimen are reported in Table 1. The samples are manufactured using a MarkTwo desktop 3D printer (Fig. 4), using the standard materials supplied by Markforged. The machine has a cartesian structure with a building volume of 320 mm × 132 mm x 154 mm.
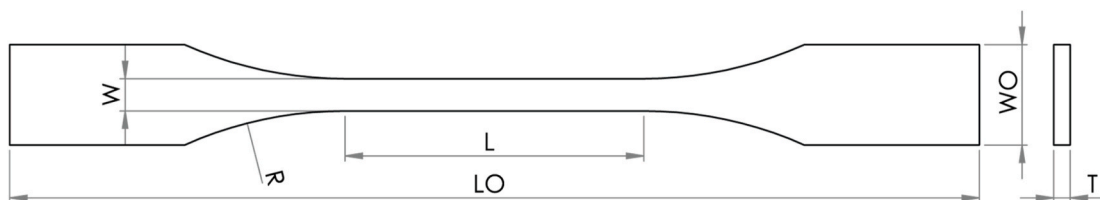

Fig. 3. Specimen geometry ASTM D638 Type II modified.

Table 1

Specimen dimensions according to ASTM D638 Type II and relative variations.

Dimensions [mm]	ASTM D638 Type II	ASTM D638 Type II - modified	Tolerances
W – Width of narrow section	6	6.1	±0.5
L – Length of narrow section	57	57	±0.5
WO – Width overall, min	19	19	+6.4
LO – Length overall, min	183	185	no max
R – Radius of fillet	76	76	±1
T – Thickness	3.2	3.125/3.1 (CF/KVF)	±0.4
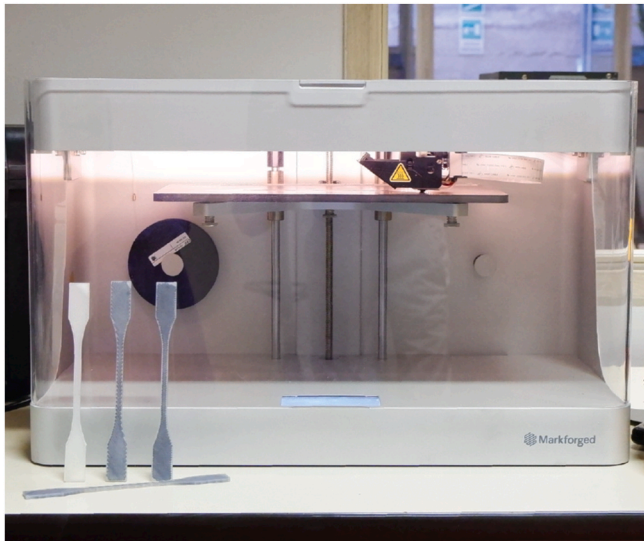
Fig. 4. MarkTwo 3D printer and a set of 4 samples used for the CF calibration model.

The manufacturing constraints of this machine are mainly related to the filament's diameter of the available materials. The height of the part must be a multiple of the layer thickness that can be set to 0.100 mm or 0.125 mm. The inner and the outer perimeter of each layer needs a minimum of 1 wall to contain the fibre filament. A minimum of 1 only matrix layer is requested, both on the bottom and top, before the reinforced layers. The temperature of the print head and the related flowrate cannot be changed. Therefore, it is not possible to use materials different from the ones supplied by Markforged.

In this work, Nylon is used for the composite matrix, whereas Carbon fibre (CF) and Kevlar fibre (KVF) are used for the reinforcement. As mentioned afore, the layer thickness depends on the fibre reinforcement material, and it is equal to 0.125 mm and 0.100 mm for CF and KVF, respectively. Owing to the manufacturing constraints of Markforged systems that pertain the deposition width and the layer thickness, the geometry of the tensile specimen needs to be slightly modified with respect to the standard design (Table 1). To this aim, the width of the narrow section is incremented by about 0.15% because the width of the deposited filament does not allow getting the exact value of the ASTM guideline. The specimen is designed to be produced with a single reinforced layer in his centre. To this aim, an odd number of layers is used. Since the thickness of the ASTM type II specimen is equal to 3.2 mm a different number of layers is used for the CF specimens and for the KVF ones. Owing to the different layer thickness imposed by Eiger settings, the specimen consists of 25 layers for the specimen reinforced with CF (0.125 mm layer) and 31 layers for the one with KVF (0.100 mm layer). Therefore, the nominal thickness of specimens is equal to 3.125 mm for

the CF ones and 3.100 mm for the KVF ones. Accordingly, the specimens in pure nylon are printed with the corresponding layer thickness to account for the differences in material properties at the macroscopic level [40]. The geometry of the specimens is modelled using SolidWorks® 2018 SP4.0 (Dassault Systèmes) and exported into the STL format. Eiger software is then used for the preparation of the build and print job. The infill strategy for the fibre is set to isotropic to get unidirectional mechanical properties of the reinforcement. The pattern is set to solid infill, and nylon layers are standardly deposited in an alternated 45° direction (Fig. 5e) with respect to the longitudinal axis of the tensile specimen. The number of walls, i.e. outer perimeter paths, is set equal to 1 to reduce the effect of matrix properties into the reinforced layer. The wall has a width corresponding to the deposited diameter of the nylon filament, which is equal to 0.4 mm, as the microscopy image (Fig. 5d) shows. According to the proposed methodology, specimens are produced with the fibre deposited at 0°, 45°, and 90° in the middle layer. Three replicas of the tensile specimen are produced for each type of reinforcement. A new print job is used for every single replica with the same machine configuration. The time to produce one specimen in nylon is 65 min for the 0.125 mm layer and 77 min in the case of the 0.100 mm layer. Although the height of the two types of sample is very similar, the higher number of thinner layers increases the production time. The time to produce the reinforced samples ranges from 74 min to 88 min. Fig. 6 shows a preview of the reinforced specimens. The reinforcement fibre is deposited continuously inside the layer area following the blue paths in Fig. 6. However, continuous deposition of the fibre does not allow to fill the entire area to be reinforced within the single layer. Therefore, empty spaces and gaps are filled by Eiger software adding a certain quantity of matrix material for which a second deposition path is computed (white paths in Fig. 6). Fig. 5a shows a printed layer reinforced with KVF deposited at 0°. The yellow filament in the image is the Kevlar fibre, while the white transparent material is nylon. The red contours highlight some area that was supposed to be filled with the reinforcement fibre to get a full composite specimen. However, since the continuous fibre is folded over itself at every inversion of the motion (turning point) of the extrusion head along the deposition path, a certain clearance is generated from the border of the reinforced area depending on the width of the fibre. The gaps in the area are automatically filled with the matrix material, according to the preview displayed by the software (white and blue paths shown against a black background in Figs. 5a and 6). Fig. 5b and c shows the presence of gaps also due to an insufficient material deposition [41].

For the sake of completeness, Fig. 6 shows the preview of all the specimens used in the experimental phase for the definition of the FE model and for its validation. In the validation phase, a set of tensile specimens are produced by depositing the fibre with three different orientations of 15°, 30° and 60° to the reference direction respectively. Three replicas are produced for each orientation and each type of fibre. Therefore, a total of 24 specimens are used for calibrating the model and additional 18 samples are tested for validating it.

After the production of the specimen, the tensile tests are performed using an AURA machine by Easydur equipped with a load cell of 10 tonnes and pneumatic wedge action grips. The strain rate for the tensile tests is set to 5 mm/min. The internal software of the machine directly records the testing data with a sampling rate of 500 Hz. All specimens are tested within a maximum of 12 h from production to avoid detrimental effects on the mechanical behaviour of the nylon matrix due to potential absorption of moisture.

5. Results and discussion

5.1. Experimental testing results

Fig. 7 shows the force-displacement curve of the three pure-nylon specimen replicas printed with 0.125 mm layer thickness. The curves present the same trend, so an excellent repeatability of the
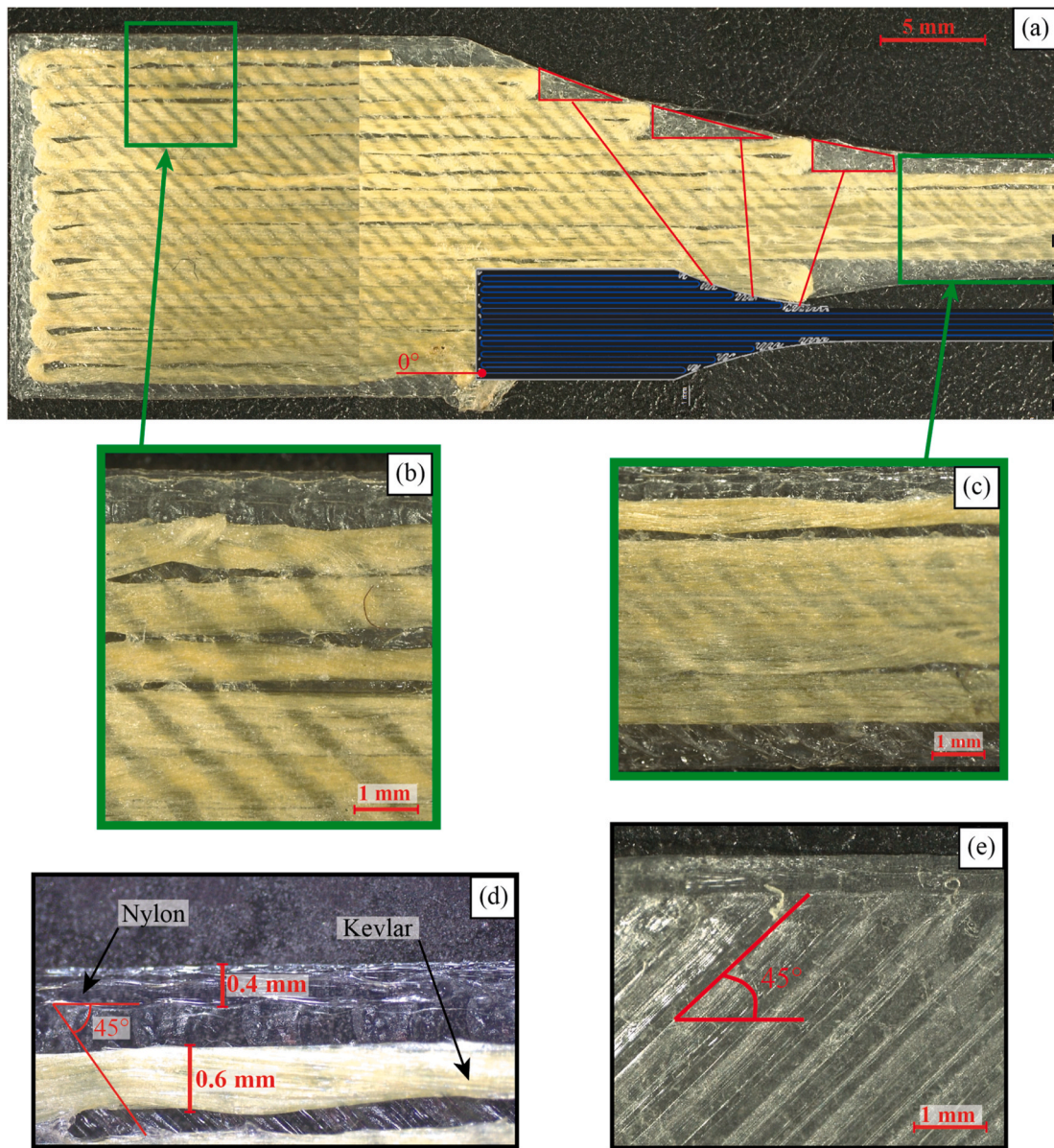
Fig. 5. Microscope images of the reinforced printed layer with the Kevlar fibre deposited at 0°. (a) The fibre is deposited along a continuous path. The turning points are visible. The empty spaces (e.g. areas with the red contour) are filled with the deposition of the matrix according to the printing preview extracted from Eiger software. (b) Detail of the deposited material in which is observed a non-constant width of the deposited fibre. (c) Detail of the deposited material in the narrow section of the specimen. (d) Detail of the deposited material in which the actual width of the wall (outer perimeter path of matrix material) of the reinforced layer and the deposited fibre are measured. The matrix layers that encapsulate the reinforced layer are deposited at 45°: (d) below and (e) on the top of the reinforced layer.

manufacturing process is observed. The repeatability is confirmed for all other printed replicas as well.

Fig. 8 illustrates the average force-displacement curves of the pure-nylon specimens printed with the two different layer thicknesses of 0.100 mm and 0.125 mm. The elongation at break of both specimens is quite high. Nevertheless, specimens with 0.125 mm layer thickness show a higher value of strength thanks to the smaller number of layers that reduce the global delamination effect. This result confirmed the previous investigations [40] about a macroscopic effect on the mechanical performance of the layer thickness.

Fig. 9 shows the force-displacement curve of the three CF specimens with the fibre oriented at 0°. The curves, which are limited to the linear behaviour, show a low dispersion and a good repeatability of the process.

Fig. 10 shows the average force-displacement curve of the specimens reinforced with the CF at different orientations. As expected, the

specimen with the fibre oriented at 0° shows the higher elastic modulus while the lower value of the modulus is observed in the case of 90° orientation of the specimen fibre. For 0° orientation, the peak of the tensile curve indicates a brittle behaviour with sudden complete fracture of the fibre. For other orientations of the reinforcement, the fibre fracture is more gradual. In the case of 90° orientation, since the tensile load acts perpendicularly to the fibre deposition, the continuous reinforcement filament is gradually unrolled during the test.

Similarly, Fig. 11 shows the force-displacement graph in the case of KVF. Compared to the CF specimens, KVF ones have higher elongation at break and lower strength. However, Kevlar fibre presents a higher impact strength [39]. This aspect influences the tensile tests and explains the increased scattering of the results at different orientations of the fibre.
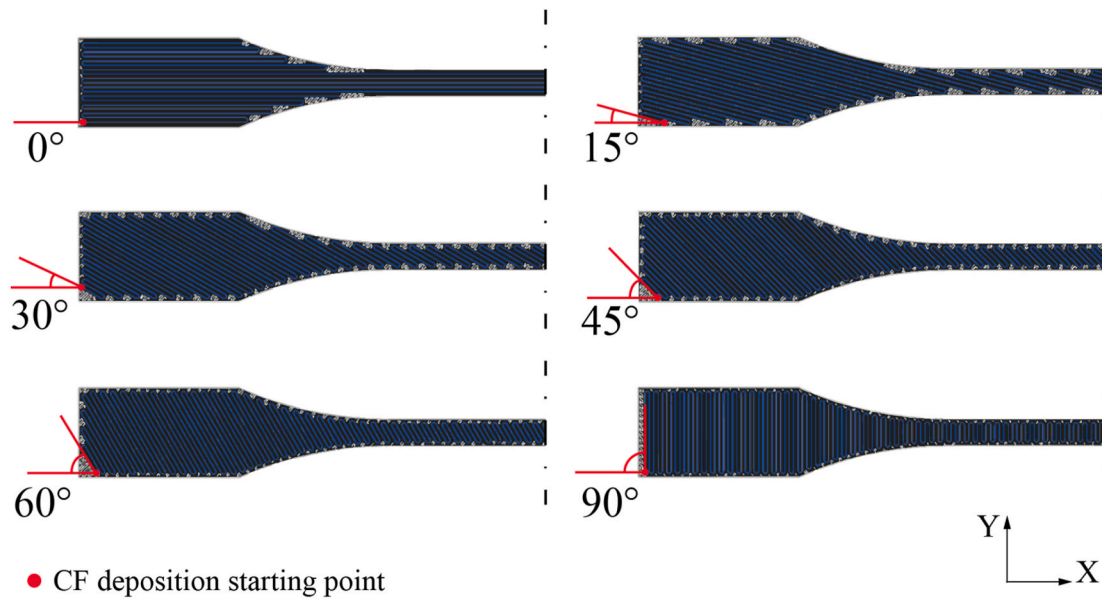
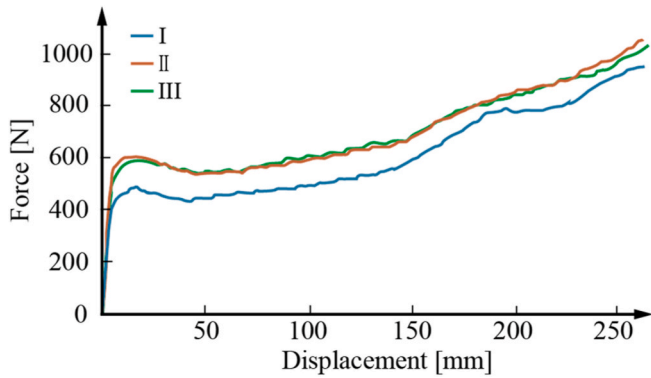**Fig. 6.** Fibre orientations of specimens.

Fig. 7. Force-displacement curve of the three pure-nylon replicas with a layer thickness of 0.125 mm.
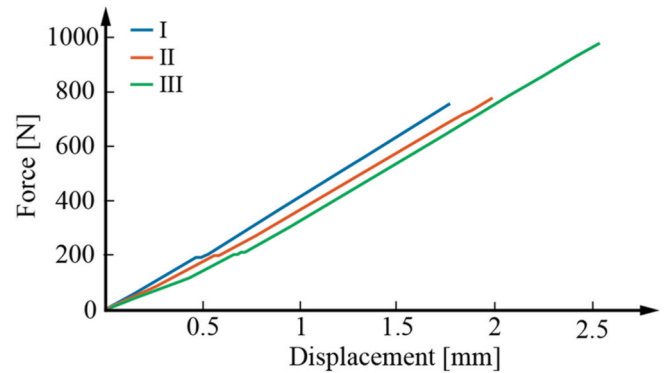

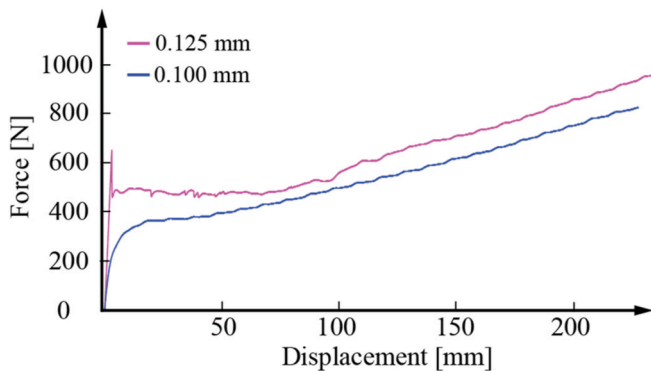**Fig. 9.** Force-displacement curve of the three CF specimen replicas with the fibre orientated at 0°.

Fig. 8. The average force-displacement curve of pure-nylon specimens with different layer thickness.
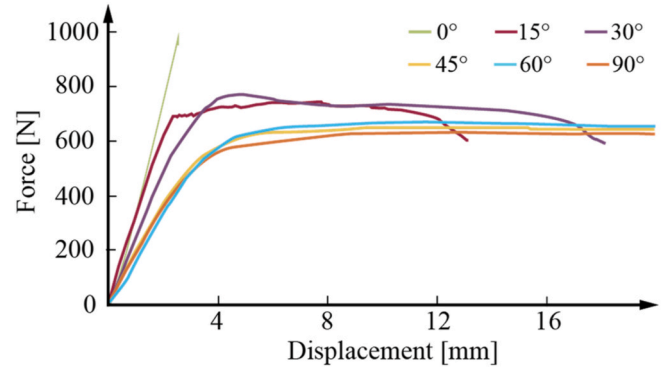

Fig. 10. The average force-displacement curve of CF specimens at different orientations.

5.2. Implementation of the FE model

The 3D finite element model is designed in Altair HyperMesh® and solved using OptiStruct®. The model aims to emulate the specimen performance, and therefore, two models are designed to consider the different layer thickness of the CF and KVF specimens. Therefore, the model includes 25 layers for CF and 31 layers for the KVF ones. Each layer, characterised by 3D Hexa- and Penta-mesh with 1 mm of maximum element size, is bonded to the adjacent ones to obtain displacement consistency. Additionally, the central layer is modelled differently to account for the nylon matrix in the perimeter surrounding the reinforcement fibre. As an example, Fig. 12 shows a cross-section of
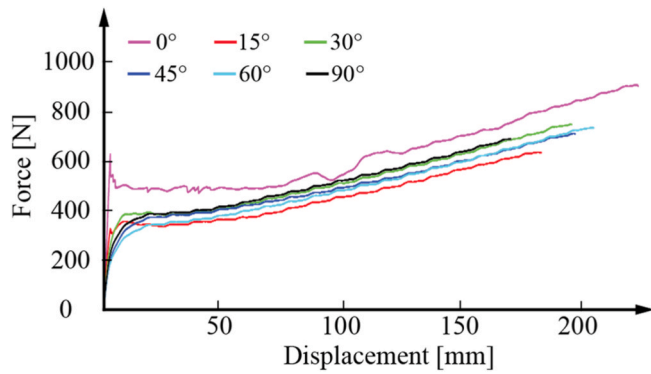
Fig. 11. The average force-displacement curve of KVF specimens at different orientations.

the model for the KVF specimen in two different planes. According to the proposed methodology, the nylon is simulated as an isotropic and homogenous material, while the reinforced layer (RF) is simulated as a homogenous and orthotropic material. The local material system is applied to each element of the RF area. For each simulation, the local material system is rotated according to the fibre orientation. The first axis of the local system is oriented along the deposition direction, the second axis is perpendicular to the deposition direction, and the third axis is perpendicular to the deposition plane. A joint constraint is set for on all nodes of the two surfaces of one of the two end-tabs to emulate the clamp. On the opposite tab, a longitudinal force is applied to an independent node of a rigid element to represent the tensile load. Fig. 12 illustrates the model schematically.

According to the proposed approach, initially, the pure nylon specimens printed at different layer thickness have been simulated. As the first attempt, the mechanical properties of the nylon are extracted from the Markforged datasheet [39] and reported in Table 2. These datasheet values are the results of the test made by Markforged Inc. according to ASTM standards without any additional specification.

To calibrate the material properties of the nylon in the FE model, the material properties are step-by-step changed until the convergence between numerical and the experimental results for both layer thicknesses. The obtained results are resumed in Table 3.

The resulting mechanical properties of the nylon are then assigned to all elements of the model to mimic the pure-nylon specimen. For the first trial, the properties of the nylon are extracted by Markforged datasheet [39] (Table 2). All calibrations are made by tuning the material

properties up to obtain the same experimental displacement corresponding to a load equal to 250 N for CF and 100 N for KVF to account for the different resistance and performance of the fibre.

The results of the calibration procedure are reported in Table 4 for CF and KVF materials. The values of the moduli of elasticity were accordingly decreased to avoid the occurrence of negative eigenvalues that generate the failure of the FE analysis.

When compared to the corresponding material properties extracted from the datasheet [39] for both the matrix and the fibres, the equivalent material proprieties which were implemented in the model are significantly different. All equivalent properties of the FE model were lower than those of the commercial datasheet for the specific material. Markforged declares that "Fiber test plaques are fully filled with unidirectional fiber and printed without walls. Plastic test plaques are printed with full infill" [39]. Under those printing conditions, the strength of the test plaques is maximized, therefore material properties on Markforged datasheets are the best values that can be achieved for the specific material in CFF. Other printing conditions and combination of the materials will reduce the mechanical performance because of the influence of the layerwise process. The lower values of the fibres can be explained by the number of pores and quantity of matrix present in the reinforced layer. Furthermore, the lower local stiffness might be due to the number of fibre breakages that occur at the turning points of the fibre deposition path [42] at the border of the layer.

Table 2
Mechanical properties by Markforged datasheet [39].

	Nylon (End of life)	Carbon	Kevlar®
Test (ASTM)	D638 type IV	D3039	D3039
Tensile Modulus [GPa]	0.94	60	27
Poisson Modulus	0.39	0.33	0.3
Shear Modulus [GPa]	0.338	22.556	10.15

Table 3
Mechanical properties of the Nylon at different layer thicknesses (lt) after the calibration.

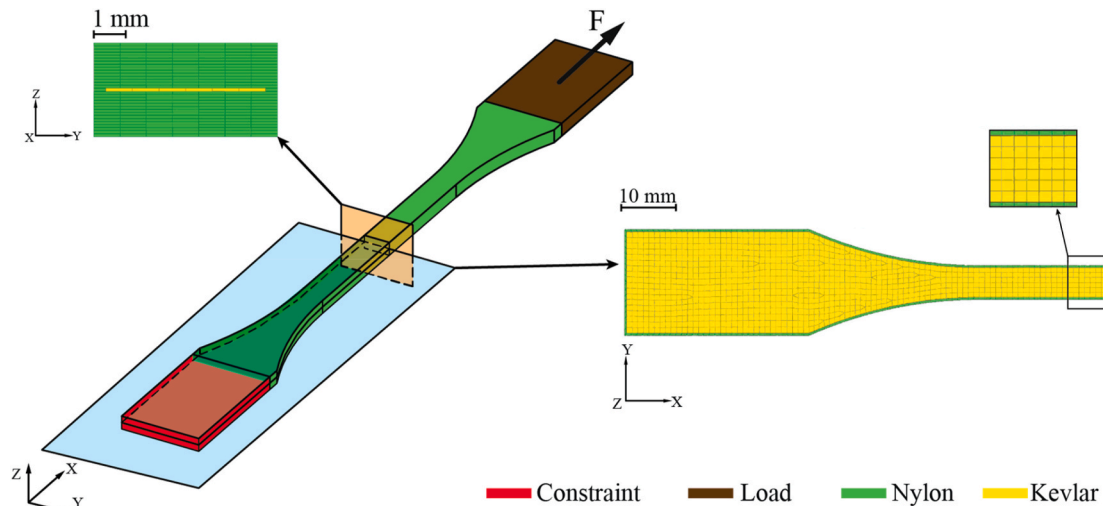|	E [GPa]	ν	G [GPa]
Nylon (from datasheet)	0.94	0.39	0.338
Nylon (lt = 0.125 mm)	0.69	0.39	0.25
Nylon (lt = 0.100 mm)	0.53	0.39	0.191

Fig. 12. FE model: middle cross-section of the KFV specimen. The red and brown domains indicate the area where the constraint and load are applied, respectively.

Table 4

Tensile properties of the for the fibre material after global convergence of the model.

	E_1 [GPa]	E_2 [GPa]	$\nu_{12} = \nu$	G_{12} [GPa]
Carbon fibre	35	7.5	0.15	4.0
Kevlar®	31	1.5	0.2	0.7

5.3. Validation

For validation purposes, the numerical force-displacement curve is computed for different loads and compared with the corresponding experimental one. Fig. 13 shows an example of a KVF specimen printed with the fibre deposited at 0°. Thanks to the previous global calibration, the numerical model represents the experimental results correctly.

The model is validated by comparing the numerical and experimental results for three new different orientations of the reinforcement fibre in the middle layer of the specimen: 15°, 30°, and 60°. Fig. 14 and Fig. 15 show this comparison for CF and KVF specimens, respectively. The model predicts the mechanical behaviour of the specimens with a good accuracy. The maximum deviation between the numerical results and the experimental ones is around 10%. The highest difference is recorded for those specimens wherein in the reinforced layer there are numerous empty areas filled by the matrix material only (e.g. 30° and 15° in Fig. 6). The additional deposited matrix material creates a higher anisotropy in the mechanical performance of the reinforced layer. The numerical error might be reduced by using a more complex FE model, that considers areas (white line in Fig. 6) with only the matrix material in the reinforced layer.

6. Conclusion

In this paper, a new approach was presented to determine the actual values of the elastic modulus that describe the mechanical behaviour of composite materials manufactured via the CCF process that belongs to additive manufacturing technologies based on material extrusion. The innovative approach is based on the use of a three-dimensional FE model, in which the properties of the printed material are homogenised and the corresponding material properties are determined and calibrated empirically using the minimum number of experimental tests only. Therefore, the so-defined material describes the printed material from a macroscopic point of view and includes the peculiarities of the CFF process thanks to the adopted empirical approach. The innovation of this model lies in the use of a local material reference system for the reinforced layer that can be rotated according to the fibre orientation. This local reference system allows simulating the mechanical behaviour of the reinforced layer in any direction. The developed model has been validated against experimental results from tensile specimens produced with the deposited fibres at three different orientations. Nevertheless, the maximum deviation between numerical and experimental values was less than 10%. This result demonstrated the validity of the presented approach. The deviation may be explained by the microscopic effect due to the presence of local areas with material properties variations. These areas are located at the border of the deposition path, where the deposition strategy (like serpentine) causes voids and sharp localised changes in the direction of fibre deposition with respect to the one considered by the model (Fig. 5a).

The equivalent material properties that emulate the macroscopic behaviour of the composite materials fabricated by CFF differed significantly from the ones claimed by the supplier, who used specimens designed to maximize test performance with zero degrees unidirectional reinforcement. Therefore, this study indicates a strong effect of the manufacturing method that must be considered during the design of the component.
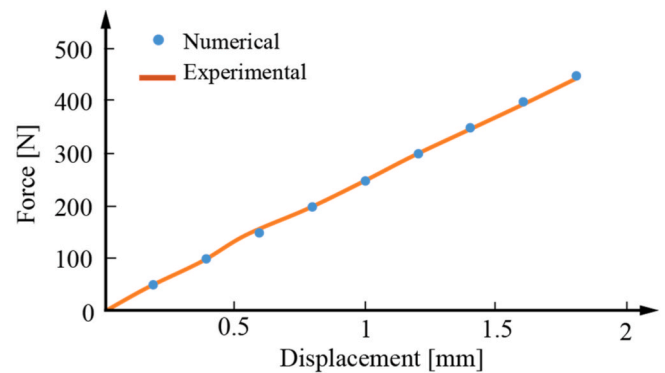

Fig. 13. Experimental and numerical force-displacement curves of the sample with Kevlar fibre deposited at 0°.
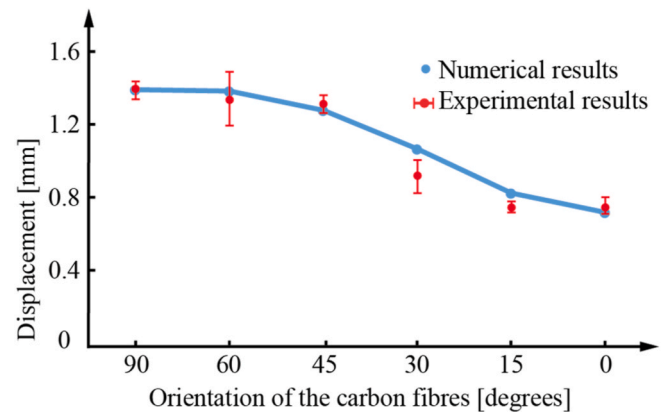

Fig. 14. Comparison between experimental and numerical displacements of specimens reinforced with Carbon fibre deposited at different orientations. The displacement corresponds to a load equal to 250 N.
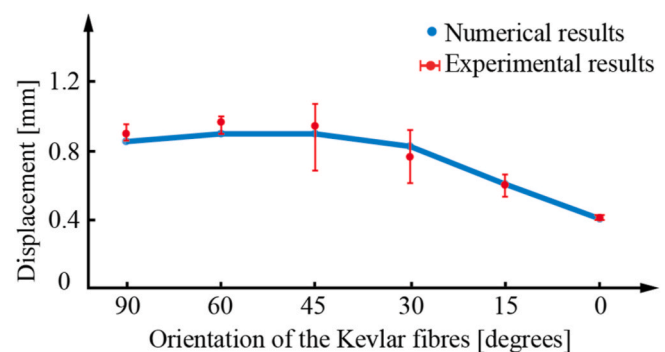

Fig. 15. Comparison between experimental and numerical displacements of specimens reinforced with Kevlar fibre deposited at different orientations. The displacement corresponds to a load equal to 100 N.

CRediT authorship contribution statement

Manuela Galati: Conceptualization, Methodology, Investigation, Writing – review & editing. **Marco Viccica:** Formal analysis, Visualization, Software, Writing – original draft. **Paolo Minetola:** Conceptualization, Resources, Writing – review & editing.

Declaration of competing interest

The authors declare that they have no known competing financial interests or personal relationships that could have appeared to influence

the work reported in this paper.

References

[1] W.D. Callister, Materials Science and Engineering: an Introduction, John Wiley& Sons, Inc. Utah, 2007.

[2] B. Xu, S. Yin, Y. Wang, H. Li, B. Zhang, R.O. Ritchie, Long-fiber reinforced thermoplastic composite lattice structures: fabrication and compressive properties, Compos. Part A Appl. Sci. Manuf. (2017), https://doi.org/10.1016/j.compositesa.2017.03.002.

[3] C. Soutis, Carbon fiber reinforced plastics in aircraft construction, Mater. Sci. Eng. 412 (2005) 171–176. https://www.sciencedirect.com/science/article/pii/S0921509305009780. (Accessed 6 September 2019).

[4] R. Stewart, Automotive composites offer lighter solutions, Reinforc Plast 54 (2010) 22–28, https://doi.org/10.1016/S0034-3617(10)70061-8.

[5] K. Challis, P. Burchill, a. Mouritz, E. Gellert, Review of advanced composite structures for naval ships and submarines, Compos. Struct. 53 (2001) 21–42.

[6] C.E. Bakis, L.C. Bank, V.L. Brown, E. Cosenza, J.F. Davalos, J.J. Lesko, A. Machida, S.H. Rizkalla, T.C. Triantafillou, Fiber-reinforced polymer composites for construction - State-of-the-art review, J. Compos. Construct. 6 (2002) 73–87, https://doi.org/10.1061/(ASCE)1090-0268(2002)6:2(73).

[7] L.C. Hollaway, The evolution of and the way forward for advanced polymer composites in the civil infrastructure, Construct. Build. Mater. 17 (2003) 365–378, https://doi.org/10.1016/S0950-0618(03)00038-2.

[8] A.B. Strong, Fundamentals of Composites Manufacturing: Materials, Methods and Applications, Society of Manufacturing Engineers, 2008.

[9] N.C. Correia, F. Robitaille, A.C. Long, C.D. Rudd, P. Šimáček, S.G. Advani, Analysis of the vacuum infusion moulding process: I. Analytical formulation, Compos. Part A Appl. Sci. Manuf. 36 (2005) 1645–1656, https://doi.org/10.1016/j.compositesa.2005.03.019.

[10] W.D. Brouwer, E.C.F.C. Van Herpt, M. Labordus, Vacuum injection moulding for large structural applications, in: Compos. Part A Appl. Sci. Manuf., Elsevier Ltd, 2003, pp. 551–558, https://doi.org/10.1016/S1359-835X(03)00060-5.

[11] D. Bender, J. Schuster, D. Heider, Flow rate control during vacuum-assisted resin transfer molding (VARTM) processing, Compos. Sci. Technol. 66 (2006) 2265–2271, https://doi.org/10.1016/j.compscitech.2005.12.008.

[12] B. Qi, J. Raju, T. Kruckenberg, R. Stanning, A resin film infusion process for manufacture of advanced composite structures, in: Compos. Struct., Elsevier Science Ltd, 1999, pp. 471–476, https://doi.org/10.1016/S0263-8223(00)00025-8.

[13] S. Wang, M. Guo, L. Yin, C. Zhou, Preliminary study of LTM resin systems and their composites, Fuhe Cailiao Xuebao(Acta Mater. Compos. Sin. 19 (2002) 28–32.

[14] N. Van De Werken, H. Tekinalp, P. Khanbolouki, S. Ozcan, A. Williams, M. Tehrani, Additively manufactured carbon fiber-reinforced composites: state of the art and perspective additively manufactured carbon fiber-reinforced composites: state of the art and perspective, Addit. Manuf. (2019), https://doi.org/10.1016/j.addma.2019.100962.

[15] F. Calignano, D. Manfredi, E.P. Ambrosio, S. Biamino, M. Lombardi, E. Atzeni, A. Salmi, P. Minetola, L. Iuliano, P. Fino, Overview on additive manufacturing technologies, Proc. IEEE 105 (2017) 593–612, https://doi.org/10.1109/JPROC.2016.2625098.

[16] D. Karalekas, K. Antoniou, Composite rapid prototyping: overcoming the drawback of poor mechanical properties, J. Mater. Process. Technol. 153–154 (2004) 526–530, https://doi.org/10.1016/j.jmatprotec.2004.04.019.

[17] J.H. Sandoval, R.B. Wicker, Functionalizing stereolithography resins: effects of dispersed multi-walled carbon nanotubes on physical properties, Rapid Prototyp. J. 12 (2006) 292–303, https://doi.org/10.1108/13552540610707059.

[18] S.H. Huang, P. Liu, A. Mokasdar, L. Hou, Additive manufacturing and its societal impact: a literature review, Int. J. Adv. Manuf. Technol. 67 (2013) 1191–1203, https://doi.org/10.1007/s00170-012-4558-5.

[19] P. Parandoush, L. Tucker, C. Zhou, D. Lin, Laser assisted additive manufacturing of continuous fiber reinforced thermoplastic composites, Mater. Des. 131 (2017) 186–195, https://doi.org/10.1016/j.matdes.2017.06.013.

[20] ASTM, Standard terminology for additive manufacturing – general principles – terminology, ASTM Int i (2015) 1–9, https://doi.org/10.1520/F2792-12A.2.

[21] W. Zhu, C. Yan, Y. Shi, S. Wen, J. Liu, Q. Wei, Y. Shi, A novel method based on selective laser sintering for preparing high-performance carbon fibres/

[22] W. Zhong, F. Li, Z. Zhang, L. Song, Z. Li, Short fiber reinforced composites for fused deposition modeling, Mater. Sci. Eng. A. 301 (2001) 125–130, https://doi.org/10.1016/S0921-5093(00)01810-4.

[23] M. Spoerk, C. Savandaiah, F. Arbeiter, G. Traxler, L. Cardon, C. Holzer, J. Sapkota, Anisotropic properties of oriented short carbon fibre filled polypropylene parts fabricated by extrusion-based additive manufacturing, Compos. Part A Appl. Sci. Manuf. (2018), https://doi.org/10.1016/j.compositesa.2018.06.018.

[24] G.T. Mark, A.S. Gozdz, Three Dimensional Printer for Fiber Reinforced Composite Filament Fabrication, 2015.

[25] M.A. Caminero, J.M. Chacón, I. García-Moreno, J.M. Reverte, Interlaminar bonding performance of 3D printed continuous fibre reinforced thermoplastic composites using fused deposition modelling, Polym. Test. 68 (2018) 415–423, https://doi.org/10.1016/j.polymertesting.2018.04.038.

[26] F. Van Der Klift, Y. Koga, A. Todoroki, M. Ueda, Y. Hirano, R. Matsuzaki, 3D printing of continuous carbon fibre reinforced thermo-Plastic (CFRTP) tensile test specimens, Open J. Compos. Mater. 6 (2016) 18–27, 2016.

[27] A.N. Dickson, J.N. Barry, K.A. McDonnell, D.P. Dowling, Fabrication of continuous carbon, glass and Kevlar fibre reinforced polymer composites using additive manufacturing, Addit. Manuf. 16 (2017) 146–152, https://doi.org/10.1016/j.addma.2017.06.004.

[28] N. Jia, H.A. Fraenkel, V.A. Kagan, Effects of moisture conditioning methods on mechanical properties of injection molded nylon 6, J. Reinforc. Plast. Compos. 23 (2004) 729–737, https://doi.org/10.1177/0731684404030730.

[29] G.R. Liu, A step-by-step method of rule-of-mixture of fiber- and particle-reinforced composite materials, Compos. Struct. 40 (1997) 313–322, https://doi.org/10.1016/S0263-8223(98)00033-6.

[30] Toray Carbon Fibers America Inc, Technical data sheet TORAYCA T300, n,d, https://www.toraycma.com/.

[31] DuPont, Kevlar Aramid fiber technical data sheet. http://www2.dupont.com/Personal_Protection/en_GB/assets/PDF/Kevlar®TechnicalGuide.pdf, 1990.

[32] G.W. Melenka, B.K.O. Cheung, J.S. Schofield, M.R. Dawson, J.P. Carey, Evaluation and prediction of the tensile properties of continuous fiber-reinforced 3D printed structures, Compos. Struct. 153 (2016) 866–875, https://doi.org/10.1016/j.compstruct.2016.07.018.

[33] ASTM, D638 – 14, Stand. Test method tensile prop, Plast 17 (2014), https://doi.org/10.1520/D0638-14.1.

[34] H. Al Abadi, H.T. Thai, V. Paton-Cole, V.I. Patel, Elastic properties of 3D printed fibre-reinforced structures, Compos. Struct. 193 (2018) 8–18, https://doi.org/10.1016/j.compstruct.2018.03.051.

[35] ASTM, Astm, D3039/D3039M-14 tensile properties of polymer matrix composite materials, Annu. Book ASTM Stand. (2014) 1–13, https://doi.org/10.1520/D3039.

[36] T.A. Dutra, R.T.L. Ferreira, H.B. Resende, A. Guimarães, Mechanical characterization and asymptotic homogenization of 3D-printed continuous carbon fiber-reinforced thermoplastic, J. Brazilian Soc. Mech. Sci. Eng. 41 (2019) 1–15, https://doi.org/10.1007/s40430-019-1630-1.

[37] A. Todoroki, T. Oasada, Y. Mizutani, Y. Suzuki, M. Ueda, R. Matsuzaki, Y. Hirano, Tensile property evaluations of 3D printed continuous carbon fiber reinforced thermoplastic composites, Adv. Compos. Mater. 29 (2020) 147–162, https://doi.org/10.1080/09243046.2019.1650323.

[38] F. Van Der Klift, 3D printed unidirectional carbon fibre reinforced polymers for aerospace applications. http://repository.tudelft.nl/, 2017.

[39] Markforged, Composites material datasheet. https://static.markforged.com/markforged_composites_datasheet.pdf%0Ahttp://static.markforged.com/downloads/composites-data-sheet.pdf, 2019.

[40] J.M. Chacón, M.A. Caminero, P.J. Núñez, E. García-Plaza, I. García-Moreno, J.M. Reverte, Additive manufacturing of continuous fibre reinforced thermoplastic composites using fused deposition modelling: effect of process parameters on mechanical properties, Compos. Sci. Technol. 181 (2019) 107688, https://doi.org/10.1016/j.compscitech.2019.107688.

[41] M. Galati, P. Minetola, On the measure of the aesthetic quality of 3D printed plastic parts, Int. J. Interact. Des. Manuf. (2019), https://doi.org/10.1007/s12008-019-00627-x.

[42] G.D. Goh, V. Dikshit, A.P. Nagalingam, G.L. Goh, S. Agarwala, S.L. Sing, J. Wei, W.Y. Yeong, Characterization of mechanical properties and fracture mode of additively manufactured carbon fiber and glass fiber reinforced thermoplastics, Mater. Des. 137 (2018) 79–89, https://doi.org/10.1016/j.matdes.2017.10.021.